Coherent transport through a ring of three quantum dots

L. Gaudreau,[1,2] A. S. Sachrajda,[1,2] S. Studenikin,[1] A. Kam,[1] F. Delgado,[1] Y. P. Shim,[1] M. Korkusinski,[1] and P. Hawrylak[1]
[1]*Institute for Microstructural Sciences, National Research Council, Ottawa, Canada K1A 0R6*
[2]*Department of Physics, University of Sherbrooke, Quebec, Canada J1K 2R1*
(Received 12 February 2009; revised manuscript received 2 July 2009; published 11 August 2009)

Low field magnetotransport measurements have been performed on a ring of three few electrons quantum dots with well-defined electron occupations. In particular detailed measurements were made at two quadruple points (where four electronic configurations are degenerate) searching for an interplay between spin-blockade mechanisms and the Aharanov-Bohm effect. Measurements were also made at neighboring triple points. An analysis of the experimental magnetotransport fast Fourier transforms (FFTs) confirms coherent transport in our device. We find, however, transport features virtually independent of the particular quantum-dot configuration in the sense that the same periods and general behavior are observed in all of the FFTs. The two dominant frequencies in the FFTs were related by a factor 3. The origin of this fractional feature in the magnetoconductance behavior is not well understood. Other even higher frequency periods also exist. All magnetoconductance periods are found to be limited by phase rigidity, confirming that their origin lies within the quantum dot circuit itself.

DOI: 10.1103/PhysRevB.80.075415 PACS number(s): 73.63.Kv, 73.23.Hk, 73.50.Dn

I. INTRODUCTION

In the current decade, research involving single and coupled electrostatic *few electron* quantum dots has been largely motivated by their potential application to the quantum-information field as spin or charge qubits. These devices also produce the opportunity to study many-body effects under controlled and tunable conditions. More recently, there has been interest in extending the complexity of these systems to triple quantum-dot arrangements. Triple quantum dots provide several opportunities not accessible in single- or double-dot systems but which are very relevant for more complex circuits. The consequences of topology,[1,2] for example, are expected to manifest themselves in triple-dot circuits. Since the exchange interaction is directly related to the tunneling properties, the topology of the interdot connectivity is predicted to play a role in determining the spin properties and indeed may provide an avenue to tune the spin properties electrically. In addition, triple quantum dots are also the simplest arrangements for implementing entanglement and encoding schemes[3–6] [N.B. ultimately the three qubit Greenberger-Horne-Zeilinger and *W* entangled states will need to be demonstrated for application to error correction schemes]. Triple quantum dots can also provide a platform for demonstrating various proposals for coherent population transfer[7,8] that will be required for critical quantum-information functionalities such as coherently busing spins around a circuit. It is important for all of these potential applications to address the question of coherent transport in these more complex circuits. In an earlier publication,[9] we provided preliminary evidence of coherent oscillations in a three dot few electron-ring potential. Aharanov-Bohm (AB) oscillations were observed by Ihn *et al.* in a ring consisting of three quantum dots containing many electrons in the cotunneling regime achieved using an alternative lithographic approach.[10] In this paper we utilize our original device to study coherent transport in a ring of three few electron quantum dots in more detail. In particular, we focus on two quadruple points with very different few electron configurations and two adjacent triple points. We find that the magnetoconductance behavior at all four points is qualitatively similar, a surprising result given the different few electron configurations involved. In addition to a sinusoidal period in the magnetoconductance, we detect a strong nonsinusoidal feature at 1/3 the period of the sinusoidal oscillations and several much higher related frequencies. Several observations commonly associated with phase rigidity (related to the two-terminal nature of the transport) in rings as well as in rings containing quantum dots are also apparent in the data.[11,12]

II. PREVIOUS MEASUREMENTS

Recently, we realized an electrostatic few electron triple quantum-dot potential where the three dots were aligned in a ring.[13] The layout of this device is usually associated with a double quantum-dot system.[14–16] Potential-profile simulations, however, confirm that this same gate layout can in principle be tuned to generate a triple-dot potential in a series arrangement. We were indeed able to use the device to switch reversibly between a double and a triple quantum-dot circuit. This specific device, however, due presumably to the underlying impurity potential, produced a triple quantum dot in a *ring* arrangement in which two dots were connected to the left lead and the third dot was connected to the right lead, as shown schematically in Fig. 1. The fundamental quadruple point (FQP) was set up and detected using charge-detection techniques.[13] At the FQP configurations (0,0,0), (0,0,1), (0,1,0), and (1,0,0) are degenerated, using the notation (N_A, N_B, and N_C), where N_i is the number of electrons in dot i. The stability diagram was mapped out in the few electron limit.[13] The important role that quantum-cellular-automata effects (QCA, i.e., system-charge rearrangements that are triggered when an electron is added to the system) play within the stability diagram in the vicinity of quadruple points was also discovered.[13] It was also found that the QCA phenomena under certain circumstances were subject to spin-

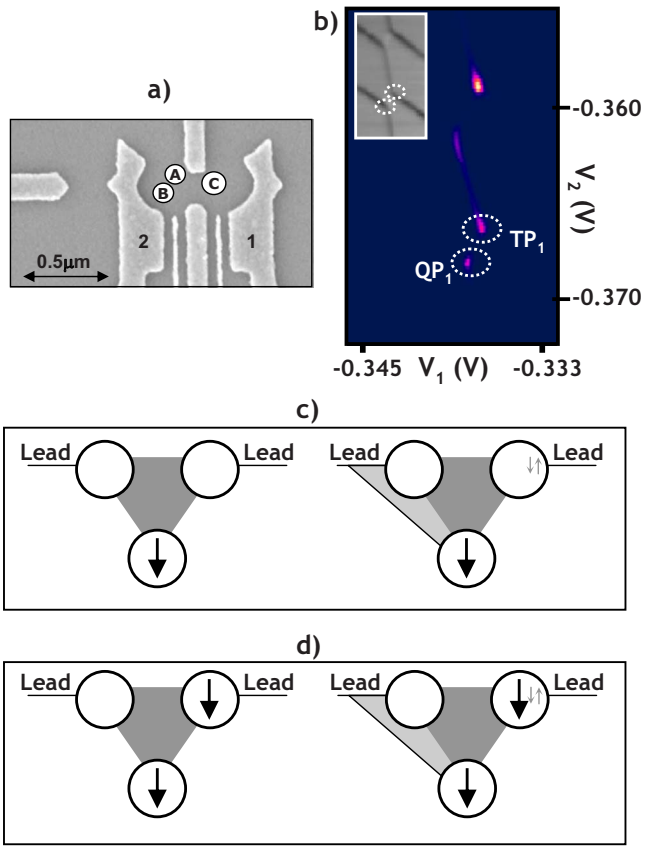

FIG. 1. (Color online) (a) SEM image of a similar device schematically indicating the position of the three quantum dots (see text for details). (b) Linear transport measurements in the V1-V2 plane at QP1 and TP1 points. Inset, the same region in the V1-V2 plane measured via charge detection indicating the QP1 and TP1 points as well as the boundaries of the different electronic configurations. (c) Schematic picture of the QP1 point where one electron is present in dot B (left) vs the actual experimental situation where the light-shaded region corresponds to an additional area enclosed between dots A, B, and the left lead, two additional electrons are located in dot C (gray arrows) in a singlet configuration (see text for details). (d) Equivalent schematic of the QP2 point where one electron resides in dot B and one in dot C (in addition to the two extra electrons).

blockade effects.[17] Soon after, Schröer *et al.* successfully realized a triple dot in series device.[18] In addition, several other realizations of triple-dots arrangements have been studied.[19–22]

III. EXPERIMENTAL DETAILS

Details of the device and the charge-detection techniques have been presented elsewhere.[13] The devices were mounted on the low-temperature end of a dilution refrigerator. While this device allowed us to reach the fundamental quadruple point for charge detection, a much more limited number of quadruple points were able to be set up for transport in the triple-dot arrangement. A further limitation was that *transport* was only detected with a minimum number of two electrons in C [see Figs. 1(c) and 1(d)].

The two quadruple points used for studying coherent transport were QP1: (0,1,2), (1,1,2), (0,2,2), and (0,1,3) and QP2: (0,1,3), (1,1,3), (0,2,3), and (0,1,4). QP1 and QP2 are related to the FQP by a (0,1,2) and (0,1,3) shift, respectively, i.e., the four degenerate configurations of QP1{2} are obtained by including (0,1,2) {(0,1,3)}, plus the three configurations generated by adding one electron to each of the three dots in turn. Furthermore, for the purpose of this discussion we make an assumption that two of the electrons in dot C occupy the lowest energy level in a singlet configuration and will not play a major role in determining any spin or transport phenomena during transport. As a result, for comparison with theory, we can expect our chosen configurations to mimic the configurations QP1* and QP2*, where QP1* and QP2* differ from the fundamental quadruple point by (0,1,0) and (0,1,1) shifts, respectively. This is illustrated in Figs. 1(c) and 1(d).

Neighboring the quadruple points within the stability diagram are associated triple points at which three configurations are degenerate. In triple quantum-dot circuits there exist two distinct categories of triple points. Conventional triple points, analogous to those that occur in two coupled dots, involve changes in the occupation of only two dots [e.g., (0,0,0), (0,1,0), and (0,0,1) where dot A is fixed, i.e., in this case empty, for every configuration]. By contrast, certain triple points only found in the vicinity of quadruple points involve configurations where no dot occupation is fixed for all three configurations—we refer to these as type-II triple points. This property is a direct consequence of the QCA effects.[13] In this paper we have studied transport at two such points; TP1 (0,1,3), (0,2,2), and (1,1,3), and TP2 (0,1,4), (0,2,3), and (1,1,4), neighboring QP1 and QP2, respectively, in addition to the quadruple points mentioned above. Transport at these points is expected to be higher order since circuit-charge rearrangements (QCA effects) are required to transfer an electron across the circuit. Strictly speaking, however, we cannot refer to this transport as cotunneling since the number of electrons in the system is not fixed.

In this work standard low and high bias low noise dc and ac techniques were employed. The device was bias cooled with +0.26 V applied to the gates to lessen switching-noise effects.[23] During the course of the measurements, periodic *relaxations* would cause the frozen-in electric field resulting from the bias cooling to lessen with a resultant increase in the amount of switching noise. As a result the experimental data around QP1 and TP1 was marginally noisier than around QP2 and TP2. This is apparent at close examination in the experimental results in this paper. In particular, to illustrate the reproducibility of the higher frequency components, we use the data taken at QP2.

To set up the desired configurations the same strategy was employed that was originally used to map out the stability diagram.[13] In particular, to achieve the quadruple points where four configurations are degenerate, the voltages were adjusted until the two relevant triple points, which were present in the stability diagram over a wide range of gate-voltage settings, fell directly on top of each other creating the quadruple configurations. For example, to set up QP1, the two triple points [(0,1,2), (1,1,2), (0,2,2)] and [(0,1,2), (0,2,2), (0,1,3)], were made to coincide via small gate opera-

tions. The type-II triple points occur automatically but only in the vicinity of certain quadruple points[24] since the relevant charge reconfigurations (QCA effects) require the energy differences between the different configurations to be small. Figure 1(b) shows the transport- and charge-detection stability diagram in the region where QP1 is set up in this way and TP1 is present. The relative amplitudes of the currents in Fig. 1(b) are dominated by the gate-voltage values and the resultant tunnel barriers to the leads, at which the points are found.

For this device, as mentioned above, the triple dot in a ring potential relied on the incidental impurity potential. In addition, while we were able to set up the required configurations, we were not able to significantly tune the interdot coupling. The tunneling values for the measurements in this paper, extracted from fitting the stability diagram are estimated to be 70 μeV between the dots A and B, and 10 μeV between dots A and C and dots B and C.[13] It is also important to note that in our device there are potentially two areas defined since two of the quantum dots (A and B) are coupled to a single lead, namely, one area encircled by the three quantum dots and another one between dots A and B and the left lead. Evidence for coherent electron injection via Aharanov-Bohm oscillations, has been previously reported in a system of two parallel quantum dots[25] connected to leads. It is, therefore, necessary to take this possibility into account when considering the data. To study coherent transport, magnetoconductance traces were taken at different points along the transport peaks in the stability diagram. The magnetoconductance measurements were performed by sweeping the magnetic field range from −0.1 to +0.1 T. It was found necessary to restrict the field sweeps to this small range as the magnetic field induced shifts in the stability diagram outside of this field-sweep window away from the quadruple points. The limited field window imposes a lower band, ~100 nm radius, on the area ($A=h/eB$) that we can theoretically detect in our coherent oscillations. Due to the incidental nature of our triple dot, it is not clear whether this field range would be sufficient to detect the predicted AB oscillations. In this paper, however, we do report the observations of periodic magnetoconductance oscillations.

IV. THEORETICAL CONSIDERATIONS

Over the last few years much has been learned about the phase diagram of a triple quantum-dot ring circuit from Hubbard-model calculations.[1,2] For one electron in a three-dot tunnel-coupled system, a *dark state* exists with zero weight in the only dot connected to the right lead, see Fig. 1(a). The appearance of these dark states can be associated with the presence of a degenerate eigenstate in the resonant triple quantum dot spectra[26] or, in specific cases, with an eigenstate with zero weight in one of the dots.[27] The influence of the dark-state configuration is expected to lead to a series of novel phenomena from quantum rectification[28] in contrast to classical rectification,[29] to coherent population-transfer applications such as spin buses via the coherent transfer via adiabatic passage protocol. A related coherent transfer population process called quantum distillation is predicted for two electrons in three dots.[30]

The *resonant* phase diagram for the triple quantum dot has been calculated.[27] In particular the two- and four-electron ground states are predicted to undergo repetitive singlet-triplet transitions as a function of magnetic field until at a sufficiently high field the triplet becomes the ground state. Three electrons are predicted to behave like a frustrated antiferromagnet ($S=1/2$) at very low fields followed by a spin-polarized phase ($S=3/2$) at higher fields. This leads to spin-blockade effects for transport experiments. For example, when $S=0$ for two electrons [at the (0,1,1), (1,1,0), (1,0,1), and (1,1,1) quadruple point], an incoming electron can make up the required spin difference to achieve $S=3/2$ for three electrons. A less extravagant behavior without spin blockade is, however, predicted for configuration QP2* [Fig. 1(b)]. Although this also involves adding a third electron to a system of two electrons just as for the resonant case in this case the ground state for three electrons is predicted to remain at $S=1/2$ at the low fields of interest for this paper while the two-electron ground state switches from 0 to 1 at a field dependant on the singlet-triplet splitting.

These theoretical calculations predict interesting transport coherent phenomena for the triple quantum-dot system. For transport through a ring of three empty quantum dots, i.e., at the FQP, a fractional AB-effect feature is predicted with a period, $T=\frac{\phi_0}{2}=\frac{h}{2eA}$, where A is the enclosed area. This effect is a direct consequence of the so-called dark state. For two or four trapped electrons, the periodicity of the energy spectrum is halved due to the appearance of total spin transitions of the ground state induced by the magnetic field.[27]

For transport through the system already containing a single (spin-up) electron an interesting interplay between the Aharanov-Bohm effect and spin blockade is predicted.[2] The theoretical charging diagram for QP1 can be seen in Fig. 1 of Ref. 2. Consider the first configuration, Fig. 1(c), illustrating QP1*. Transport occurs when a bias is applied and a second electron is added to the circuit. If the ground state of two electrons is a singlet, a spin-down electron will enter the system from the spin unpolarized leads. It can take either the lower or upper path and transport will result in AB oscillations. On the other hand, if the ground state of the system is a triplet state, we might intuitively expect the AB oscillations to be suppressed (and calculations confirm this effect[2]) since the electron will avoid the lower path due to spin blockade. Since the theoretically predicted behavior for two electrons in a triple quantum dot involves episodic singlet-triplet transitions as a function of magnetic field, we may expect the AB oscillations to be periodically suppressed in a magnetic field. At even higher fields the AB oscillations will be totally suppressed due to the transition to the triplet ground state. Furthermore, the diamagnetic shift induced by the magnetic field moves the system away from the quadruple point.[27] Calculations also reveal that for reasonable parameters (e.g., lead to dot couplings weaker than interdot couplings) the presence of a second area would only dampen the AB oscillations.

V. EXPERIMENTAL RESULTS AND DISCUSSIONS

The fundamental experimental observations can be summarized as follows: (i) FFTs at each of the locations at which

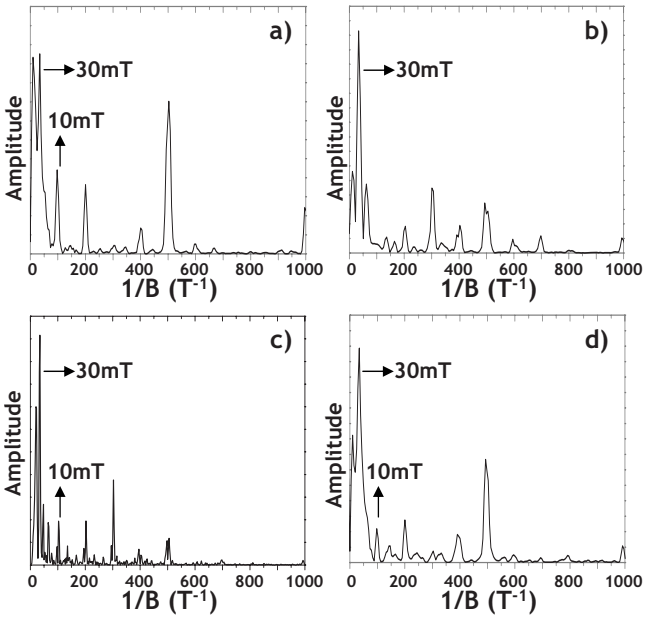

FIG. 2. FFT of magnetotransport measurements through (a) TP1, [(b) and (c)] two points on the TP2 peak (see text for details), and (d) QP1, showing the predominant periods in magnetic field.

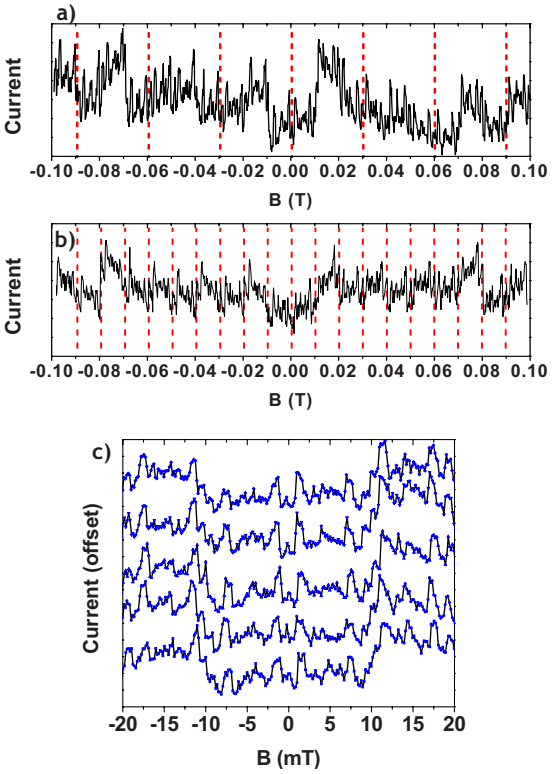

FIG. 3. (Color online) (a) Magnetotransport measurements at point TP2 showing the 30 mT period (vertical lines at 30 mT period have been superimposed as a guide to the eye). (b) Magnetotransport measurements at point QP1 where a nonsinusoidal 10 mT period can be discerned (vertical red lines at that period are shown as a guide to the eye). (c) Zoom of several sweeps at point TP2 showing the reproducibility of the high-frequency component in the magnetotransport.

measurements were made reveal a qualitatively similar behavior in contrast to configuration specific results that might be expected based on the theoretical considerations above; (ii) Periodic magnetoconductance oscillations are observed as the temperature is lowered below 700 mK. However, the behavior is more complex than the expected AB oscillations with several related magnetoconductance periods revealed in the FFTs. In particular, a strong nonsinusoidal component is observed at one third of the dominant sinusoidal period; (iii) Effects associated with phase rigidity related to the two-terminal nature of the measurements are observed for all of the periods in the FFTs. These latter effects confirm that the coherent transport originates directly within the triple quantum-dot circuit even though the extracted areas are many times the size of the quantum-dot circuit.

Figure 2 shows examples of FFTs at different points in the stability diagram. It can clearly be seen from the FFT spectrum that similar behavior occurs at these points. There exists a main peak at 30 mT corresponding to an effective radius, r, of 200 nm ($\pi r^2 = \frac{h}{e\Delta B}$). While this area fits into our lithographic device, it is larger than expected when gate-depletion distances are considered. We note, however, that in this experiment the relevant area is not rigidly defined unlike, for example, a narrow "ring." In another experiment where the relevant AB area was internal to a quantum dot[31] a correction term to the change in flux, i.e., $B\Delta A$ in addition to the usual $A\Delta B$, was invoked where A was the change in area realized during the addition of one flux quantum. Not surprisingly a first harmonic peak corresponding to a period of 15 mT is frequently observed. The most dramatic result in the data, however, is the peak at 10 mT (the third harmonic) accompanied by many harmonically related peaks of this 10 mT period. The most significant harmonic of the 10 mT peak in the data is usually at 2 mT (500 T^{-1}).

Although the FFTs confirm the presence of multiple periods in every measurement (i.e., at all locations and voltage position along the peaks), the individual periods can frequently be seen in the magnetoresistance traces. Figures 2(b) and 2(c) are both at TP2 but taken at slightly different positions on the transport peak. In Fig. 2(b) the 10 mT peak is suppressed unlike Fig. 2(c). This allows us to highlight an interesting and clear difference between the nature of the 10 and 30 mT periods whenever these two periods are independently visible in the data. In Fig. 3 examples are plotted where the 30 and 10 mT can be independently discerned. The 30 mT period [Fig. 3(a)] [using the data from Fig. 2(b)] has a sinusoidal form while the 10 mT period (taken at QP1) possesses a sawtooth, fanolike, and oscillation shape (N.B. the nonsinusoidal nature partially explains the presence of so many harmonics of the 10 mT period in the FFTs). We stress that the high-frequency component in the data is highly reproducible when the background noise level is low enough. This is illustrated in Fig. 3(c) where several sweeps are taken over a small field range to highlight the 2 mT period.

In order to confirm that these high-frequency periods originate from the quantum-dot circuit and not from the leads, we now demonstrate that all frequency components have properties similar to those observed in experiments on quantum rings containing barriers or quantum dots in one arm of the ring. These properties are often referred to as phase-rigidity[11] effects. Similar effects in ballistic transport

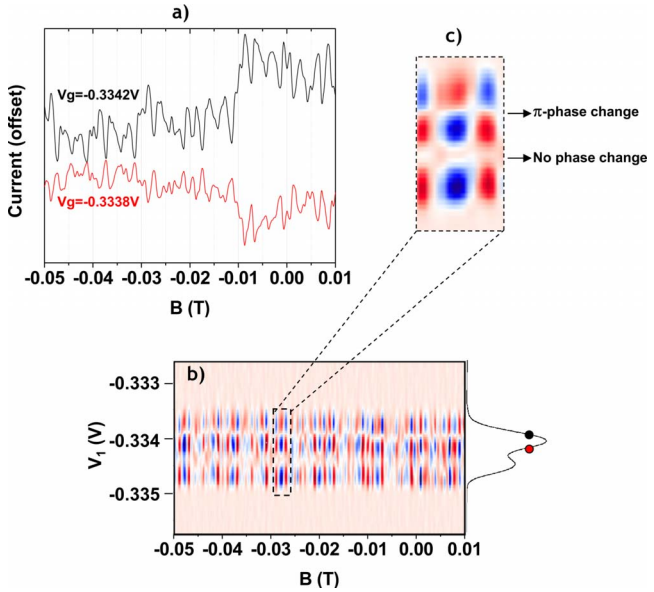

FIG. 4. (Color online) (a) Magnetotransport measurements at point QP2 in the high-bias regime. Each trace was taken at two different points of the transport peak, a π-phase difference is observed between the two runs. (b) Numerical derivative (dI/dB) across the whole transport peak [shown on the right-hand side of the graph at 0 T, the black and red points on the curve correspond to the traces in (a)]. (c) Zoom of a region in (b) showing the visibility modulations in the magnetotransport followed by a π-phase change and no phase change.

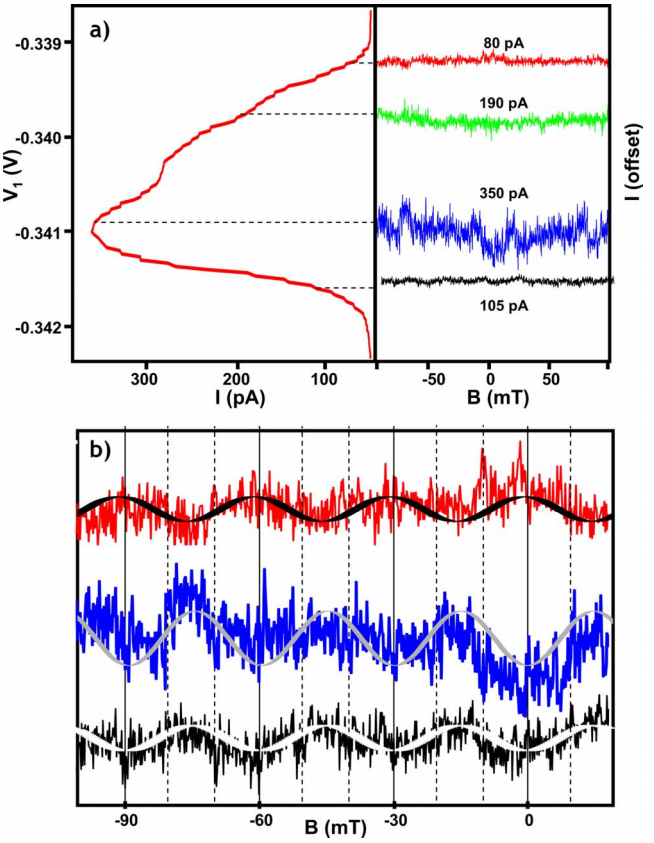

FIG. 5. (Color online) (a) Magnetotransport measurements at point QP1 in a high-bias regime (300 μV). The left panel shows the transport peak as a function of gate voltage at 0 T in the high-bias regime (current is shown on the x axis). The right panel corresponds to the magnetic field behavior of the current on different points of the transport peak from the left panel (linked by dashed lines). (b) Zoom of the selected curves in (a) showing a 30 mT period (sinusoidal lines superimposed for clarity) with a π-phase difference between the black and red curves. In the blue curve the 30 and 10 mT periods can be seen by eye to coexist.

have also been observed.[32] Due to reciprocity, all two terminal measurements, such as the ones in this paper, must be symmetric around $B=0$ T, thereby ensuring either a peak or a trough at $B=0$ T. Experiments on quantum rings containing either tunable barriers or quantum dots in one arm of the ring have revealed several experimental consequences of phase rigidity. These include (a) a quenching of the oscillation visibility while π-phase changes occur in the oscillations as a barrier is activated in one arm of the ring, (b) a span of the double frequency Altshuler-Aronov-Spivak oscillations in the low-visibility regime, (c) occasional π-phase changes as the bias across the ring is increased, and (d) π-phase changes on sweeping through a quantum-dot level. A more complex phase behavior is revealed in related experiments performed outside the phase-rigid regime, i.e., four terminal measurements, in the few electron limit.[33]

Phase-rigid effects similar to those observed in quantum dots are observed in all of our frequency components. This is illustrated in Figs. 4–6. Figure 4 plots data at QP2 for the high-frequency components. As mentioned above, telegraph noise was largely absent in QP2 and TP2 measurements allowing very detailed measurements on the high-frequency components. The double-peak structure [Fig. 4(b)] is due to the application of a 30 μV bias. The peak marks the transition from (0,1,3) to (0,2,3). However, on the quadruple point, peak configurations (1,1,3) and (0,1,4) are also degenerate. The two curves in Fig. 4(a) are magnetoresistance measurements taken at the blue and red points on either side of one of the peaks. It can be seen that the two curves are virtually identical except for a π-phase shift. Figure 4(b) plots the field derivative of the magnetoconductance across the peak. To illustrate the behavior more clearly, Fig. 4(c) plots a zoom of part of the data. Two visibility oscillations can be seen corresponding to sweeping through the two peaks. One involves a π-phase shift while the second, interestingly, has no phase shift, in contrast to previous measurements on a single-quantum dot in a ring. The observation that sweeping

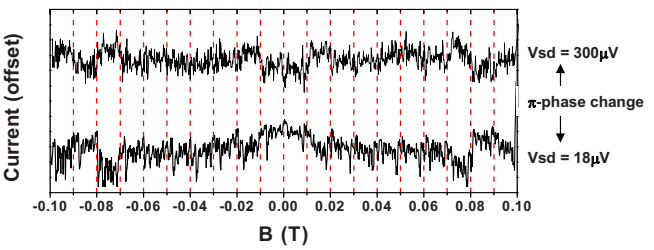

FIG. 6. (Color online) Magnetotransport measurements at point TP1 in the low- and high-bias regime showing a π-phase difference depending on the bias (dashed lines at 10 mT period shown as a guide to the eye).

through the quantum-dot resonance causes visibility oscillations and phase shifts in the high-frequency components, confirms that their origin lies in the triple quantum-dot circuit and not in the leads. Figure 5 plots related data for the 30 mT period at QP1. The broad peak in Fig. 5(a) is taken with a high bias across the device at QP1. The curves plotted on the right-hand side are magnetoconductance traces taken at various locations of this transport peak. The top and bottom curves from Fig. 5(a) are replotted with a finer amplitude scale as the top and bottom curves in Fig. 5(b). A clear 30 mT period and π shift is visible. The second curve from the top in Fig. 5(a) is taken at a visibility oscillation where the magnetoconductance oscillations are quenched. The third curve in Fig. 5(a) is plotted as the middle curve in Fig. 5(b). Figure 6 plots magnetoresistance traces taken at low and high bias at TP1. The 10 mT period is clearly visible in the low bias trace. While this is more difficult to resolve in the high bias trace, it is clearly apparent that a π-phase change has occurred.

The data and the theory do agree on the presence of magnetoconductance oscillations but clearly do not agree on the details. This is not totally surprising since quantitatively the predicted behavior is based on an intricate interplay between the tunnel couplings, Zeeman energy scale, dot sizes, and temperature. Experimentally, the small tunnel coupling between dot C and the other two dots (close to our measurement resolution) would result in a very small singlet-triplet splitting and would make it highly unlikely that we would be able to resolve the interesting theoretical effects predicted. As mentioned above, since two of the quantum dots are coupled to the same lead, it is possible to have a second parallel area if there is coherent injection of electrons from the leads to the quantum dots. Extensive modeling has been therefore performed to see if an additional area could generate the extra frequencies in the FFTs under the condition that the coupling between the dots themselves was stronger than between the leads and the dots. It was found that indeed extra peaks could be observed in FFTs and that by choosing exactly equal areas, peaks in the FFT related by a factor 3 could be generated. However, further details of the FFT and the very specific line-shape behavior described above could not be reproduced, confirming that any effect due to the possible second area for electrons being transmitted through the quantum-dot circuit was highly unlikely to be the origin of the rich observations. While the origin of the small period oscillations is not understood, the fact that they appear in all triple and quadruple points studied suggest that a possible explanation based on QCA is quite unlikely. We also note that the presence of the two extra electrons in dot C has not been taken into account in the modeling and the assumption that they do not play a role in the results remains to be verified theoretically and experimentally. Interestingly, there has been a previous observation of a fractional AB effect in few electrons quantum rings but only under conditions of weak coupling to the leads,[34] i.e., weak screening of the electron-electron interactions. While the similarity of a triple quantum dot at a quadruple point and a few electron quantum ring is suggestive of a common origin, it is not clear how the specific theoretical explanations which were successfully invoked to explain the quantum ring results and were based specifically on the one-dimensional ring nature of the device could be adapted to the present experiment.

VI. CONCLUSIONS

In conclusion we have studied coherent transport through a triple quantum dot in a ring arrangement. Magnetotransport measurements were made at quadruple and triple points in the stability diagram at which interesting interplays might be expected between spin blockade and the AB effect. A complex magnetoconductance effect was observed. In particular, in addition to the expected low-frequency sinusoidal behavior, much higher frequencies were also observed. The higher frequencies were shown to originate from the quantum-dot circuit through the observation of a series of phase-rigidity effects. The origin of the higher frequency components remain to be explained.

ACKNOWLEDGMENTS

We acknowledge the expert assistance of Piotr Zawadzki in the measurements and useful conversations with Aash Clerk, Mona Berciu, and Frank Wilhelm. A.S.S. and P.H. acknowledge funding from NSERC and CIFAR.

[1] M. Korkusinski, I. P. Gimenez, P. Hawrylak, L. Gaudreau, S. A. Studenikin, and A. S. Sachrajda, Phys. Rev. B **75**, 115301 (2007).
[2] F. Delgado, Y.-P. Shim, M. Korkusinski, L. Gaudreau, S. A. Studenikin, A. S. Sachrajda, and P. Hawrylak, Phys. Rev. Lett. **101**, 226810 (2008).
[3] D. P. DiVincenzo, D. Bacon, J. Kempe, G. Burkard, and K. B. Whaley, Nature (London) **408**, 339 (2000).
[4] P. Hawrylak and M. Korkusinski, Solid State Commun. **136**, 508 (2005).
[5] D. S. Saraga and D. Loss, Phys. Rev. Lett. **90**, 166803 (2003).
[6] D. M. Greenberger, M. A. Horne, and A. Zeilinger, *Bell's Theorem, Quantum Theory, and Conceptions of the Universe* (Kluwer Academic, New York, 1989).
[7] A. D. Greentree, J. H. Cole, A. R. Hamilton, and L. C. L. Hollenberg, Phys. Rev. B **70**, 235317 (2004).
[8] K. Eckert, M. Lewenstein, R. Corbalán, G. Birkl, W. Ertmer, and J. Mompart, Phys. Rev. A **70**, 023606 (2004).
[9] L. Gaudreau, A. S. Sachrajda, S. Studenikin, P. Zawadzki, A. Kam, and J. Lapointe, in *Physics of Semiconductors*, edited by W. Jantsch and F. Schaffler, AIP Conf. Proc. No. 893 (AIP, New York, 2007), p. 857.
[10] T. Ihn, M. Sigrist, K. Ensslin, W. Wegscheider, and M. Reinwald, New J. Phys. **9**, 111 (2007).
[11] A. Yacoby, M. Heiblum, D. Mahalu, and H. Shtrikman, Phys. Rev. Lett. **74**, 4047 (1995).

[12] A. Yacoby, R. Schuster, and M. Heiblum, Phys. Rev. B **53**, 9583 (1996).
[13] L. Gaudreau, S. A. Studenikin, A. S. Sachrajda, P. Zawadzki, A. Kam, J. Lapointe, M. Korkusinski, and P. Hawrylak, Phys. Rev. Lett. **97**, 036807 (2006).
[14] J. M. Elzerman, R. Hanson, J. S. Greidanus, L. H. Willems van Beveren, S. De Franceschi, L. M. K. Vandersypen, S. Tarucha, and L. P. Kouwenhoven, Phys. Rev. B **67**, 161308(R) (2003).
[15] M. Pioro-Ladrière, R. Abolfath, P. Zawadzki, J. Lapointe, S. A. Studenikin, A. S. Sachrajda, and P. Hawrylak, Phys. Rev. B **72**, 125307 (2005).
[16] J. R. Petta, A. C. Johnson, J. M. Taylor, E. A. Laird, A. Yacoby, M. D. Lukin, C. M. Marcus, M. P. Hanson, and A. C. Gossard, Science **309**, 2180 (2005).
[17] L. Gaudreau, A. S. Sachrajda, S. A. Studenikin, P. Zawadzki, and A. Kam, Physica E (Amsterdam) **40**, 978 (2008).
[18] D. Schroer, A. D. Greentree, L. Gaudreau, K. Eberl, L. C. L. Hollenberg, J. P. Kotthaus, and S. Ludwig, Phys. Rev. B **76**, 075306 (2007).
[19] M. C. Rogge and R. J. Haug, Phys. Rev. B **77**, 193306 (2008).
[20] K. Grove-Rasmussen, H. I. Jørgensen, T. Hayashi, P. E. Lindelof, and T. Fujisawa, Nano Lett. **8**, 1055 (2008).
[21] S. Amaha, T. Hatano, S. Teraoka, A. Shibatomi, S. Tarucha, Y. Nakata, T. Miyazawa, T. Oshima, T. Usuki, and N. Yokoyama, Appl. Phys. Lett. **92**, 202109 (2008).
[22] S. Amaha, T. Hatano, T. Kubo, Y. Tokura, D. G. Austing, and S. Tarucha, Proceedings of the 17th International Conference on Electronic Properties of Two-Dimensional Systems, Genova, Italy, 2007, edited by G. Goldoni and L. Sorba [Physica E (Amsterdam) **40**, 1322 (2008)].
[23] M. Pioro-Ladrière, J. H. Davies, A. R. Long, A. S. Sachrajda, L. Gaudreau, P. Zawadzki, J. Lapointe, J. Gupta, Z. Wasilewski, and S. Studenikin, Phys. Rev. B **72**, 115331 (2005).
[24] L. Gaudreau, A. S. Sachrajda, S. Studenikin, P. Zawadzki, J. Lapointe, and A. Kam, Phys. Status Solidi C **3**, 3757 (2006).
[25] A. W. Holleitner, C. R. Decker, H. Qin, K. Eberl, and R. H. Blick, Phys. Rev. Lett. **87**, 256802 (2001).
[26] F. Delgado and P. Hawrylak, J. Phys.: Condens. Matter **20**, 315207 (2008).
[27] F. Delgado, Y.-P. Shim, M. Korkusinski, and P. Hawrylak, Phys. Rev. B **76**, 115332 (2007).
[28] B. Michaelis, C. Emary, and C. W. J. Beenakker, Europhys. Lett. **73**, 677 (2006).
[29] A. Vidan, R. M. Westervelt, M. Stopa, M. Hanson, and A. C. Gossard, Appl. Phys. Lett. **85**, 3602 (2004).
[30] J. Fabian and U. Hohenester, Phys. Rev. B **72**, 201304(R) (2005).
[31] B. J. van Wees, L. P. Kouwenhoven, C. J. P. M. Harmans, J. G. Williamson, C. E. Timmering, M. E. I. Broekaart, C. T. Foxon, and J. J. Harris, Phys. Rev. Lett. **62**, 2523 (1989).
[32] R. P. Taylor, A. S. Sachrajda, J. A. Adams, C. R. Leavens, P. Zawadzki, and P. T. Coleridge, Superlattices Microstruct. **11**, 219 (1992).
[33] M. Avinun-Kalish, M. Heiblum, O. Zarchin, D. Mahalu, and V. Umansky, Nature (London) **436**, 529 (2005).
[34] U. F. Keyser, C. Fühner, S. Borck, R. J. Haug, M. Bichler, G. Abstreiter, and W. Wegscheider, Phys. Rev. Lett. **90**, 196601 (2003).